

PAPER • OPEN ACCESS

Non-invasive studies of multiphase flow in process equipment. Positron emission particle tracking technique

To cite this article: B V Balakin *et al* 2017 *J. Phys.: Conf. Ser.* **781** 012039

View the [article online](#) for updates and enhancements.

Related content

- [Direct Numerical Simulation of Multiphase Flows with Unstable Interfaces](#)
Eugenio Schillaci, Oriol Lehmkuhl, Oscar Antepara *et al.*
- [Positron scattering from Biomolecules](#)
J R Machacek, W Tattersall, R A Boadle *et al.*
- [Characterization of the latest Birmingham modular positron camera](#)
T W Leadbeater, D J Parker and J Gargiuli

Non-invasive studies of multiphase flow in process equipment. Positron emission particle tracking technique

B V Balakin^{1,2}, T C H Adamsen^{3,4}, Y-F Chang², P Kosinski² and A C Hoffmann²

¹ Bergen University College, Department of Mechanical and Marine Engineering, Norway

² University of Bergen, Department of Physics and Technology, Norway

³ University of Bergen, Department of Chemistry, Norway

⁴ Haukeland University Hospital, Department of Nuclear Medicine, Norway

E-mail: boris.balakin@hib.no

Abstract. Positron emission particle tracking (PEPT) is a novel experimental technique for non-invasive inspection of industrial fluid/particle flows. The method is based on the dynamic positioning of a positron-emitting, flowing object (particle) performed through the sensing of annihilation events and subsequent numerical treatment to determine the particle position. The present paper shows an integrated overview of PEPT studies which were carried out using a new PET scanner in the Bergen University Hospital to study multiphase flows in different geometric configurations.

1. Introduction

Positron emission particle tracking (PEPT) is a modification of the well-known positron emission tomography (PET) method widely employed in nuclear medicine. Both techniques combine sequential detection of back-to-back gamma-rays resulting from a positron/electron annihilation event with advanced mathematical post-processing of a sensing log. A typical PET system therefore requires the positioning of a positron-emitting isotope within a set of gamma-detectors, e.g. scintillators, distributed in space in a way allowing detection of gamma-rays from a single annihilation event. The detectors are integrated in a PET-scanner unit where their output is collected and pre-analysed by advanced hardware in a data-processing controller. The classical PET technique is primarily focused on the registration of annihilation events from spatial regions where a β^+ -emitter is distributed and the subsequent image reconstruction, while PEPT defines a point source of β^+ performing cross-triangulation directly from a sensing log of individual "lines of response" (LORs). A LOR is a line drawn between two sensors of the scanner, which detect photons emitted from the same annihilation event, i.e. a double-detection must be performed within a very narrow temporal gap. In principle, the point of intersection of multiple LORs is recognized in PEPT as the spatial position of the point radioactivity source, however, in practise a number of factors lead to some spatial scatter in the LORs [1]. Due to relatively high energy of gamma-rays (511 keV), they are able to penetrate a wide range of industrial surfaces opaque to visible light, PEPT is therefore suitable for non-invasive control of industrial equipment where



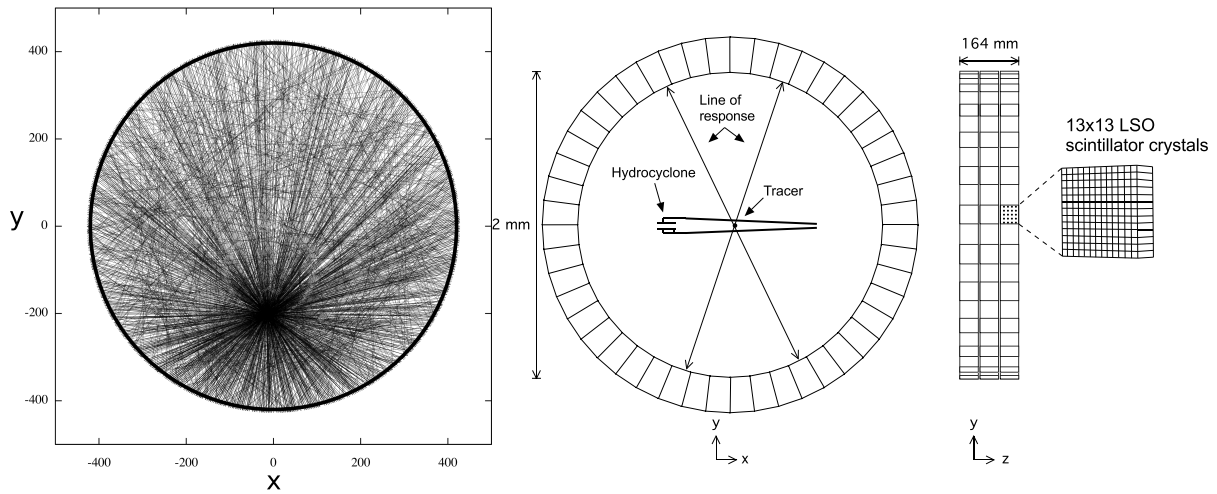


Figure 1. Left: LORs from a tracer particle registered by the camera in 1 ms in a 2D cross-section of camera. Right: the hydrocyclone located in the PET scanner.

direct visual access to the flow is impossible [2]. Comparing basic principles of PET and PEPT it can be concluded that the later operates with a precise and compact dataset which results in far better spatial and temporal resolution for the position of a point source.

The first records on PEPT experiments come from the University of Birmingham [3] where the technique was used to elucidate flow in rotating drums [4], stirred vessels [5], turbines [6], casting [7], paste flows [8] and solid-liquid flow systems [9]. The technique was subsequently adopted by different research groups reporting studies of fluidized beds [10], granulators [11] and other process equipment. The in-situ PEPT-study of an industrial multiphase system by PEPT was reported by Ingram et al. [12]. The present paper provides a detailed overview of the PEPT experiments performed at the PET center of Haukeland University Hospital (Norway) to explore pneumatic conveying lines and hydrocyclones at the conditions similar to industrial.

2. Materials and methods

The experiments were conducted with the use of Siemens TruePoint medical PET scanner with the energetic detection interval 425-650 keV. The scanner, presented schematically in Fig. 1 (right), comprises three 855.2-mm detecting rings. Each ring is equipped with 48 sensor blocks combined of 13×13 lutetium oxyorthosilicate (LSO) scintillator crystals with the size $4 \times 4 \times 20$ mm. The blocks are separated in radial and axial directions by one crystal gap so the axial depth of the detection zone is 164 mm. The co-incidence time of a single-LOR detection is set to 4.5 ns [2], so that if two photons are detected within this window, they are assumed to emanate from one annihilation event. An example of the LORs from 1 ms reconstructed from a stationary emitter of positrons in presented in Fig. 1 (left). It can be seen in the figure that, in addition to the afore-mentioned scatter, there is a certain number of "false" LORs appear due to a random co-incidence, multiple co-incidence and Compton interaction [2].

Multiphase flow was studied in the two types of processing systems: a tangential-inlet 414-mm length hydrocyclone with a diameter of 40 mm (Fig. 3(left)) and a vertical 50-cm cylindrical PVC-pipeline section for pneumatic conveying with the diameter of 45.2 mm combined with two $50 \times 88.5^\circ$ bends and a replaceable flow straightener of the honeycomb/mixing-plate type (Fig. 4). The carrier phase in case of the hydrocyclone was water, in some cases with dissolved NaCl, resulting in a density of 1100 kg/m^3 intended to match that of the tracer particle and therefore to study the flow of the fluid in the hydrocyclone; and air at normal conditions in the case of the

pneumatic conveying study. The test equipment was connected to flow loops comprising flow agitators (centrifugal pump and gas compressor) generating continuous flow through the test sections of the loop in the field of view of the camera, dispersed phase injectors, flow meters and a system of by-pass lines. The details of the flow loops design may be found elsewhere [2, 13].

The dispersed phase, and, in the case of the neutral-density tracer particle, the continuous phase, was represented by the tracer particles emitting positrons. Amberlyst anion-exchange styrene divinylbenzene beads with the mean size $430 \pm 56 \mu\text{m}$ and average density 1070 kg/m^3 , shown in Fig. 2, were used. The beads were labelled with ^{18}F ($t_{1/2} = 110 \text{ min}$) as follows: at first a sample of 0.5 ml of water was exposed by protons in cyclotron establishing $^{18}\text{O}(\text{p},\text{n})^{18}\text{F}$ nuclear reaction, the beads are then immersed into the resulting radioactive solution and agitated there for 10 minutes until ^{18}F is adsorbed by the bead material via the ion-exchange mechanism; the bead, with the individual activity up to $2000 \mu\text{Ci}$, is then removed from the solution, dried with a filter paper and injected into the flow.

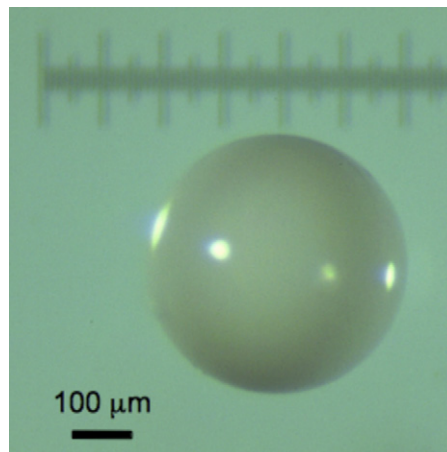


Figure 2. Amberlyst A21 anion exchange resin bead

The position of the tracer in the flow of the carrier phase is detected using the algorithm originating from Hoffmann et al. [1]. The algorithm initially detects all the LORs and the two-dimensional (x - y) co-ordinates of their intersections are determined from the sensor positions obtained in the 64-bit list-mode log files from the PET scanner. The average of all the intersection coordinates is computed and outlying intersections eliminated, which first are those intersections generated by "false" LORs. The rest of the intersection coordinates are averaged again and the procedure of eliminating outliers and narrowing the spatial averaging window is repeated until only intersections remain that are within a final spatial window with a diameter below 20 mm [2]. The final position of the tracer is found by averaging the intersections located in this window. Optimization of the size of the final window is done by verifying that this size results in the lowest standard deviation of the positions of a stationary tracer. The coordinate of the particle in the third dimension is obtained by averaging of the intersection between the remaining LORs from the last dataset. The computational costs may further be reduced assuming the first window to be located in the vicinity of the tracer position at the previous time step. The first window is centered on the position minimizing the sum of the squared distances to all of the LORs, an analytical expression for this position was derived.

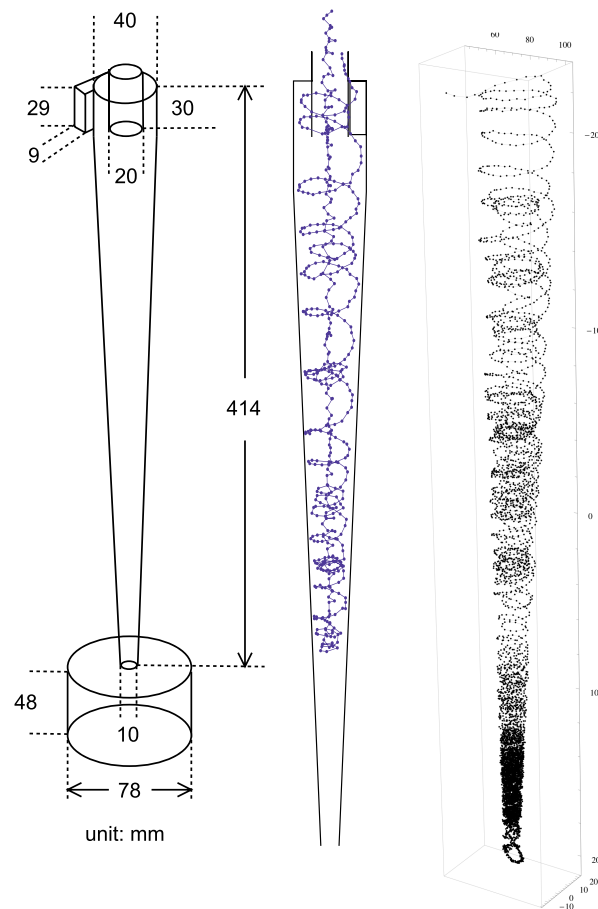


Figure 3. Left: dimensions of the hydrocyclone. Middle: Track of a neutral-density particle after 505 ms with very low residual activity, inlet flow velocity 3.6 m/s. Right: track of a tracer particle larger than the cyclone cut-size in water with a position recorded every 500 μ s.

3. Results and discussion

The trajectory of a neutral-density tracer in the hydrocyclone at $Re=158\,400$ is presented in Fig. 3 (middle), where the points represent the particle position with an acquisition step of 1.0 ms. As is seen in the figure, the particle enters the cyclone and, instead of flowing smoothly to the underflow close to the wall of the cyclone, as would be expected for a solid particle larger than the cut-size of the separator, it quickly starts moving radially in and out due to the turbulence in the flow. Low in the cyclone it reverses the direction of its axial velocity, moving into the inner, upwardly flowing, vortex and moves out through the liquid outlet in the cyclone roof following the liquid flow. The solid particle in water, to the right in the figure, represents the behaviour of a particle larger than the cut-size of the cyclone. This track is of the normal high quality since the activity remains on the particle and it is feasible to determine a position every 500 μ s. One would expect such a particle to move smoothly to the particle outlet in the bottom of the cyclone. However, it can be seen to take several excursions into the inner vortex of upwardly directed flow on the way. This is unexpected, and is an effect that can only be observed with Lagrangian particle tracking. Moving further downwards the conical section of the cyclone, the particle experiences significant deviations from the swirling motion, probably due to the presence of the “end of the vortex” at this position, where the vortex end is attached to the wall and precesses resulting in the generation of a complex fluid flow pattern and a less-than-optimal downward

particle transport. Under this position, a swirling motion is restored, albeit very much weaker, induced by the precessing of the vortex. In the experiments [2], the density of the tracer particle was matched by adding salt to the fluid in order to study the flow of the fluid in the cyclone. This proved very challenging, however, since the activity leached from the particle very quickly, leading to tracking under difficult conditions, and the development of post-processing methods to reduce the resulting high scatter [2]. The second experimental system, presented in Fig. 4

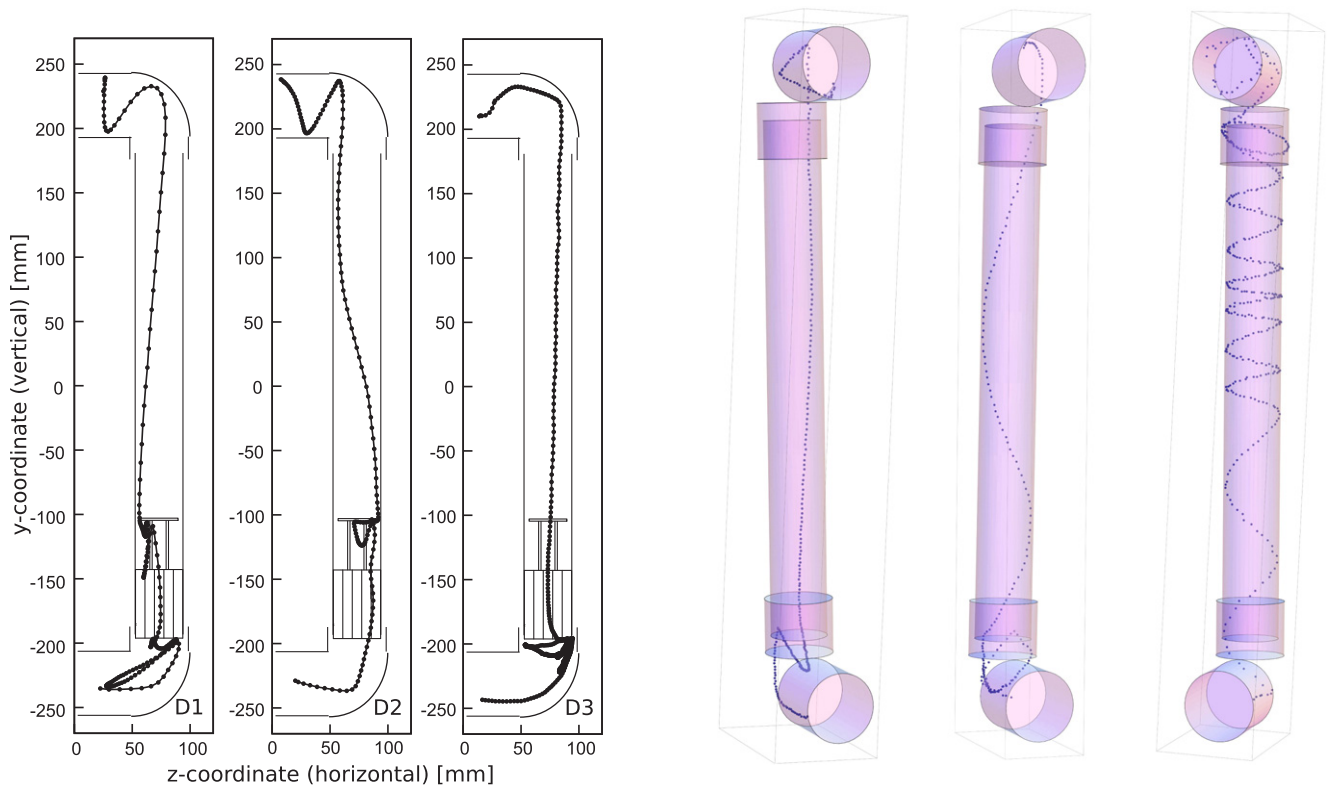


Figure 4. Particle tracks obtained in the pneumatic system. Left: interaction of the tracer with the flow straightener in 2D projection at 15.7, 10.6, 4.4 m/s (left→right). Right: 3D tracks in an obstacle-free section at 5.0, 16.9 and 17.1 m/s (left→right).

demonstrates the particle behaviour in a pneumatic conveying system with (left) and without (right) a flow straightener installed at Reynolds numbers in the interval 10500–41500. First we focus on the system with flow straightener where tracks are presented for mean flow velocities of 15.7, 10.6 and 4.4 m/s. As it can be observed in the figure, the tracer is approaching the test section moving nearly horizontally and experiences multiple reflections from the straightener elements with magnitudes proportional to the flow velocity. The reflections, which take place with a coefficient of restitution of 0.81 [14], give rise to reversed motion of the particle. The fluid and particle phases are only weakly coupled (the particle Stokes number is in the range 48–187). The particulate phase flow after the straightener becomes aligned over the rest of the test section and experiences rotational motion caused by the formation of asymmetrical Dean vortices (one vortex becomes dominant) formed in the carrier phase after the second bend.

It is further possible to observe from the 3-D images to the right in Fig. 4 that a spiral-like motion of the tracer is induced in some cases in the test section when the straightener is removed. As in the cyclonic case in the conical section, the frequency of the swirling motion increases with the mean flow velocity. This might be expected, taking into account possible

interference of Dean vortices at higher Re . Although the particles experience minor reflections from the elements forming the bend, they do not affect the swirling motion. The particle tracks are rather insensitive to gravity at the Reynolds numbers selected, while the influence of electrostatic forces potentially induced on the tracer due to friction with plastic walls could be considered as possible. It is finally reasonable to conclude that the flow straightener conditions the upward flow better than the empty elbow.

4. Conclusions

The present paper illustrates the behaviour of multiphase flow in two types of process equipment: the hydrocyclone and the pneumatic system with obstacles, captured by means of positron emission particle tracking. This paper and ref. [2] demonstrate that the technique is able to visualise the behaviour of both the carrier phase, making the tracer neutrally buoyant in the carrier fluid, or the flow of the inertial dispersed phase where other forces than the drag become important. The temporal resolution of the technique is 1 ms or better while the spatial resolution is determined by the inherent scatter, the activity on the tracer particle and the sophistication of the algorithm used to position the particle. The technique is non-invasive and the algorithm analysing the PET scanner logs takes less than 60 min on an ordinary PC. This method is therefore suitable for the benchmarking of numerical models [15]. PEPT is applicable to most types of the process equipment which is confirmed by other studies performed by our group for the dispersion in Hartmann tube [14] and the liquid-solid flow in a recirculated flow loop [15].

5. Acknowledgments

The authors would like to thank Jan Selbu and Øyvind Steimler at Haukeland University Hospital for their support during the experiments.

References

- [1] Hoffmann A C, Dechsiri van de Wiel C F, Dehling H G PET investigation of a fluidized particle: spatial and temporal resolution and short term motion 2005 *Measurement Science and Technology* **16** 851–858
- [2] Chang Y F, Ilea C G, Aasen Ø L, Hoffmann A C Particle flow in a hydrocyclone investigated by positron emission particle tracking 2011 *Chemical Engineering Science* **66** 4203 – 4211
- [3] Parker D J, Hawkesworth M R, Broadbent C, Fowles P, Fryer T D, McNeil P A Industrial positron-based imaging: Principles and applications 1994 *Nuclear Instruments and Methods in Physics Research Section A: Accelerators, Spectrometers, Detectors and Associated Equipment* **348** 583–592
- [4] Ding Y L, Forster R, Seville J P K, Parker D J Segregation of granular flow in the transverse plane of a rolling mode rotating drum 2002 *International Journal of Multiphase Flow* **28** 635 – 663
- [5] Barigou M, Fan X, Parker D, Nienow A, Guida A Positron emission particle tracking in a mechanically agitated solid-liquid suspension of coarse particles 2009 *Chemical Engineering Research and Design* **87** 421–429
- [6] Fishwick R P, Winterbottom J M, Parker D J, Fan X F, Stitt E H Hydrodynamic measurements of up-and down-pumping pitched-blade turbines in gassed, agitated, vessels using positron emission particle tracking 2005 *Industrial and Engineering Chemistry Research* **44** 6371–6380
- [7] Griffiths W D, Beshay Y, Parker D J, Fan X The determination of inclusion movement in steel castings by positron emission particle tracking (PEPT) 2008 *Journal of Materials Science* **21** 6853–6856
- [8] Wildman R D, Blackburn S, Benton D M, McNeil P A, Parcker D J Investigation of paste flow using positron emission particle tracking 1999 *Powder Technology* **103** 220–229
- [9] Fairhurst P, Barigou M, Fryer P, Pain J-P, Parker D Using positron emission particle tracking (PEPT) to study nearly neutrally buoyant particles in high solid fraction pipe flow 2001 *International Journal of Multiphase Flow* **27** 1881 – 1901
- [10] Chan C W, Seville J, Fan X, Baeyens J Solid particle motion in a standpipe as observed by positron emission particle tracking 2009 *Powder Technology* **194** 58 – 66
- [11] Schaafsma S, Marx T, Hoffmann A Investigation of the particle flowpattern and segregation in tapered fluidized bed granulators 2006 *Chemical Engineering Science* **61** 4467 – 4475
- [12] Ingram A, Hausard M, Fan X, Parker D J, Seville J P K, Finn N, Kilvington R, Evans M Portable positron

- emission particle tracking (PEPT) for industrial use 2007 *Proceedings of 12th International Conference on Fluidization* 13–17
- [13] Middha P, Balakin B V, Leirvaag L, Hoffmann A C, Kosinski P, PEPT - a novel tool for investigation of pneumatic conveying 2013 *Powder Technology* **237** 87 – 96
- [14] Berg A E Investigation of dust dispersion in a modified Hartmann tube. Master Thesis (under consideration) *the University of Bergen* 2016
- [15] Ghaffari M, Chang Y-F, Balakin B, Hoffmann A C CFD modelling of PEPT results of particle motion trajectories in a pipe over an obstacle 2012 *AIP Conference proceedings* **1479** 193–196